Relational Graph Transformer

Vijay Prakash Dwivedi[1]   **Sri Jaladi**[1]   **Yangyi Shen**[1]   **Federico López**[2]
Charilaos I. Kanatsoulis[1]   **Rishi Puri**[3]   **Matthias Fey**[2]   **Jure Leskovec**[1,2]
[1]Stanford University,   [2]Kumo.AI,   [3]NVIDIA
{vdwivedi,jure}@cs.stanford.edu

Abstract

Relational Deep Learning (RDL) is a promising approach for building state-of-the-art predictive models on multi-table relational data by representing it as a heterogeneous temporal graph. However, commonly used Graph Neural Network models suffer from fundamental limitations in capturing complex structural patterns and long-range dependencies that are inherent in relational data. While Graph Transformers have emerged as powerful alternatives to GNNs on general graphs, applying them to relational entity graphs presents unique challenges: (i) Traditional positional encodings fail to generalize to massive, heterogeneous graphs; (ii) existing architectures cannot model the temporal dynamics and schema constraints of relational data; (iii) existing tokenization schemes lose critical structural information. Here we introduce the Relational Graph Transformer (RELGT), the first graph transformer architecture designed specifically for relational tables. RELGT employs a novel multi-element tokenization strategy that decomposes each node into five components (features, type, hop distance, time, and local structure), enabling efficient encoding of heterogeneity, temporality, and topology without expensive precomputation. Our architecture combines local attention over sampled subgraphs with global attention to learnable centroids, incorporating both local and database-wide representations. Across 21 tasks from the RelBench benchmark, RELGT consistently matches or outperforms GNN baselines by up to 18%, establishing Graph Transformers as a powerful architecture for Relational Deep Learning[1].

1 Introduction

Real-world enterprise data, such as financial transactions, supply chain data, e-commerce records, product catalogs, customer interactions, and electronic health records, are predominantly stored in relational databases [8]. These databases typically consist of multiple tables, each dedicated to different entity types, interconnected through primary and foreign key links. This abstraction underpins large quantities of complex, dynamically updated data that scale with business volume, storing potentially immense, unexploited knowledge [13]. However, extracting predictive patterns from such data has traditionally depended on manual feature engineering within complex machine learning pipelines, requiring the transformation of multi-table records into flat feature vectors suitable for models like deep neural networks and decision trees [6].

Relational Deep Learning. To enable end-to-end deep learning, relational databases can be represented as relational entity graphs [13], where nodes correspond to entities and edges capture primary-foreign key relationships. This graph-based representation allows Graph Neural Networks (GNNs) to learn abstract features directly from the underlying data structure, effectively modeling complex dependencies for various downstream prediction tasks. With this setup, which is termed as Relational Deep Learning (RDL), GNNs reduce or eliminate the need for manual feature engineering and often lead to improved performance [42], at a fraction of the traditional model development cost.

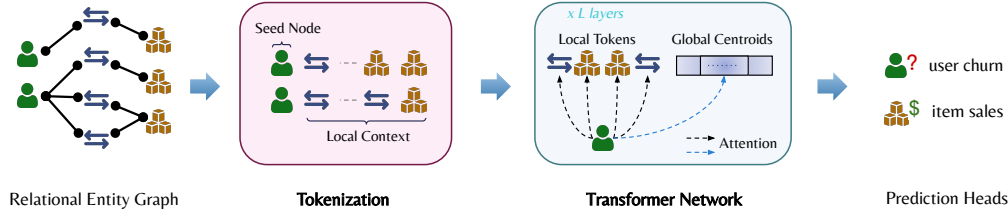[1]https://github.com/snap-stanford/relgt

Preprint.

Figure 1: Overview of the RELGT architecture. First, the input relational entity graph (REG) is converted into tokens where each training seed node (such as the *customer* node in this example) gets a fixed number of neighboring nodes, which are encoded with a multi-element tokenization strategy. These tokens are then passed through a Transformer network that builds both local and global representations, which are then fed to downstream prediction layers.

Existing gaps. Despite their effectiveness, standard message-passing GNN architectures [15, 29, 18, 48] have notable limitations, such as insufficient structural expressiveness [52, 37, 34] and restricted long-range modeling capabilities [1]. For example, consider an e-commerce database with three tables: *customers*, *transactions*, and *products*, which can be represented as a relational entity graph as in Figure 1. In a standard GNN, *transactions* are always two hops away from each other, connected only through shared customers. This creates an information bottleneck: *transaction*-to-*transaction* patterns require multiple layers of message passing, while *product* relationships remain entirely indirect in shallow networks. Furthermore, *products* would never directly interact in a two-layer GNN [42], as their messages must pass through both a transaction and a customer, highlighting the inherent structural constraints of GNN architectures that restrict capturing long-range dependencies.

Graph Transformers (GTs) have emerged as more expressive models for graph learning, utilizing self-attention in the full graph to increase the range of information flow and additionally, incorporating positional and structural encodings (PEs/SEs) to better capture graph topology [9, 53, 41]. These advances have produced strong results across domains [38], including foundation models for molecular graphs [46]. However, many GT designs are limited to non-temporal, homogeneous, and small-scale graphs, assumptions that do not hold for relational entity graphs (REGs) [13], which are typically (i) heterogeneous, with different tables representing distinct node types; (ii) temporal, with entities often associated with timestamps and requiring careful handling to prevent data leakage; (iii) large-scale, containing millions or more records across multiple interconnected tables. In particular, existing PEs often require precomputation, depend on graph size, and typically do not scale well to large, heterogeneous, or dynamic graphs [3, 26]. For instance, node2vec [17], while more efficient than Laplacian or random walk PEs, can become prohibitively expensive and impractical to compute on massive graphs [40]. These limitations, along with the inability to capture the multi-dimensional complexity of relational structures, render current GTs inadequate for relational databases.

Present work. We introduce the **Relational Graph Transformer (RELGT)**, the first Graph Transformer specifically designed for relational entity graphs. RELGT addresses key gaps in existing methods by enabling effective graph representation learning within the RDL framework. It is a unified model that explicitly captures the temporality, heterogeneity, and structural complexity inherent to relational graphs. We summarize the architecture as follows (Figure 1):

- **Tokenization:** We develop a multi-element tokenization scheme that converts each node into structurally enriched tokens. By sampling fixed-size subgraphs as local context windows and encoding each node's features, type, hop distance, time, and local structure, RELGT captures fine-grained graph properties without expensive precomputation at the subgraph or graph level.

- **Attention:** We develop a transformer network that combines local and global representations, adapting existing GT architectures [41]. The model extracts features from the local tokens while simultaneously attending to learnable global tokens that act as soft centroids, effectively balancing fine-grained structural modeling with database-wide patterns [30].

- **Validation:** We showcase RELGT's effectiveness through a comprehensive evaluation on 21 tasks from RelBench [42]. RELGT consistently outperforms GNN baselines, with gains of up to 18%, establishing transformers as a powerful architecture for relational deep learning. Compared to HGT [20], a strong GT baseline for heterogeneous graphs, RELGT achieves better results without added computational cost, even when HGT uses Laplacian eigenvectors for positional encoding.

2

2 Background

2.1 Relational Deep Learning

Relational Deep Learning (RDL) is an end-to-end representation learning framework that converts relational databases into graph structures, enabling neural networks to be applied directly and eliminating the need for manual feature extraction in multi-table data pipelines [13].

Definitions. Formally, we can define a **relational database** as the tuple (T, R) comprising a collection of tables $T = \{T_1, \ldots, T_n\}$ connected through inter-table relationships $R \subseteq T \times T$. A link $(T_{\text{fkey}}, T_{\text{pkey}}) \in R$ denotes a foreign key in one table referencing a primary key in another. Each table contains entities (rows) $\{v_1, \ldots, v_{n_T}\}$, with each entity typically consisting of: (1) a unique identifier (primary key), (2) references to other entities (foreign keys), (3) entity-specific attributes, and (4) timestamp information indicating when the entity was created or modified. The structure of relational databases inherently forms a graph representation, called as **relational entity graphs** (REGs). An REG is formally defined as a heterogeneous temporal graph $G = (V, E, \phi, \psi, \tau)$, where nodes V represent entities from the database tables, edges E represent primary-foreign key relationships, ϕ maps nodes to their respective types based on source tables, ψ assigns relation types to edges, and τ captures the temporal dimension through timestamps [13].

Challenges. Relational entity graphs exhibit three distinctive properties that set them apart from conventional graph data. First, their structure is fundamentally schema-defined, with topology shaped by primary-foreign key relationships rather than arbitrary connections, creating specific patterns of information flow that require specialized modeling approaches. Second, they incorporate temporal dynamics, as relational databases track events and interactions over time, necessitating techniques like time-aware neighbor sampling to prevent future information from leaking into past predictions. Third, they display multi-type heterogeneity, as different tables correspond to different entity types with diverse attribute schemas and data modalities, presenting challenges in creating unified representations that effectively integrate information across diverse node and edge types [44, 49]. These characteristics create both challenges and opportunities for GNN architectures, requiring models that can simultaneously address temporal evolution, heterogeneous information, and schema-constrained structures while processing potentially massive multi-table datasets.

2.2 RDL Methods

The baseline GNN approach introduced by [42] for RDL uses a heterogeneous GraphSAGE [18] model with temporal-aware neighbor sampling, which demonstrates significant improvements compared to traditional tabular methods like LightGBM [27] across all tasks in the RelBench benchmark. This baseline architecture leverages PyTorch Frame's multi-modal feature encoders [19] to transform diverse entity attributes into initial feature embeddings that serve as input to the GNN. Several specialized architectures have been developed to address specific challenges in relational entity graphs. RelGNN [5] introduces composite message-passing with atomic routes to facilitate direct information exchange between neighbors of bridge and hub nodes, commonly found in relational structures. Similarly, ContextGNN [55] employs a hybrid approach, combining pair-wise and two-tower representations, specifically optimized for recommendation tasks in RelBench.

Beyond pure GNN approaches, retrieval-augmented generation techniques [51] and hybrid tabular-GNN methods [32] have also demonstrated comparable or slightly superior performance to the standard GNN baseline, while showing the use of LLMs [16] and inference speedups, respectively. These approaches confirm the effectiveness of graph, tabular, and LLM-based methods for downstream predictions in relational databases. However, these methods typically optimize specific aspects of the problem, failing to incorporate broader advances from GTs in general graph learning.

2.3 Graph Transformers

Graph Transformers extend the self-attention mechanism from sequence modeling [47] to graph-structured data, offering powerful alternatives to traditional GNNs [9]. These models typically restrict attention to local neighborhoods, functioning as message-passing networks with attention-based aggregation [24, 2], while positional encodings are developed based on Laplacian eigenvectors [10]. Subsequent Graph Transformers incorporate global attention mechanisms, allowing all nodes to

3

attend to one another [53, 36, 31]. This moves beyond the local neighborhood limitations of standard GNNs [1], albeit at the cost of significantly increased computational complexity.

Modern GT architectures have improved the aforementioned early works by creating effective structural encodings and ensuring scalability to medium and large-scale graphs. For structural expressiveness of the node tokens, several positional and structural encoding methods have been developed [12, 3, 33, 22, 26] to inject the input graph topology. For scalability, various strategies have emerged including hierarchical clustering that coarsens graphs [57, 59], sparse attention mechanisms that reduce computational cost [41, 45], and neighborhood sampling techniques for processing massive graphs [58, 4, 30, 11]. Models like GraphGPS [41] combine these advances through hybrid local-global designs that maintain Transformers' global context advantages while ensuring practical efficiency when scaling to medium and large graph datasets. However, these approaches exhibit several key limitations: they are largely confined to static graphs, and lack mechanisms to handle multiple node and edge types. While specialized Transformers for heterogeneous graphs exist [20, 35, 59, 56], integrating them, alongside other aforementioned methods, into the RDL pipeline remains challenging. This is primarily because adapting positional encodings under precomputation constraints is difficult, compounded by the complexity of modeling large-scale, temporal, and heterogeneous relational entity graphs (REGs).

3 RELGT: Relational Graph Transformer

3.1 Tokenization

Traditional Transformers in natural language processing represent text through tokens with two primary elements: (i) **token identifiers** (or features) that denotes the token from a vocabulary set and (ii) **positional encodings** that represent sequential structure [47]. For example, a token can correspond to a word and its positional encoding can correspond to its order in the input sentence. Similarly, Graph Transformers *generally* adapt this two-element representation to graphs, where nodes are tokens with features, and graph positional encodings provide structural information [9, 28, 41]. Although this two-element approach works well for homogeneous static graphs, it becomes computationally inefficient when trying to encode multiple aspects of graph structural information for REGs.

In particular, capturing heterogeneity, temporality, and schema-defined structure (as defined in Section 2.1) through a single positional encoding scheme would either require complex, multi-stage encoding or result in significant information loss about the rich relational context. For instance, if we were to extend existing PEs for REGs, several practical challenges emerge: (i) standard Laplacian or random walk-based PEs would need significant modification to differentiate between multiple node types (*e.g.*, customers vs. products vs. transactions), (ii) these encodings lack mechanisms to incorporate temporal dynamics critical for time-sensitive predictions (*e.g.*, capturing that a user's recent purchases are more relevant than older ones), and (iii) the scale of relational databases makes global PE computation in REGs prohibitively expensive. With millions of records across tables, precomputation would only be feasible on small subgraphs, resulting in incomplete structural context.

3.1.1 Proposed Approach

RELGT overcomes these limitations through a multi-element token representation approach, without any computational overhead concerning the dependency on the number of nodes in the input REG. Rather than trying to compress all structural information into a single positional encoding, we decompose the token representation into distinct elements that explicitly model different aspects of relational data. This decoupled design allows each component to capture a specific characteristic of REGs: node features represent entity attributes, node types encode table-based heterogeneity, hop distance preserves relative distances among nodes in a local context, time encodings capture temporal dynamics, and GNN-based positional encodings preserve local graph structure.

Sampling and token elements. The tokenization process in RELGT converts a REG $G = (V, E, \phi, \psi, \tau)$ into sets of tokens suitable for processing by the Transformer network. Specifically, as shown in Figure 2, for each training seed node $v_i \in V$, we first sample a fixed set of K neighboring nodes v_j from within 2 hops of the local neighborhood using temporal-aware sampling[2],

---

[2] When fewer than K neighbors are available within 2 hops, we use randomly selected nodes as fallback tokens to maintain the fixed size K, ensuring consistent computational complexity regardless of local structure.
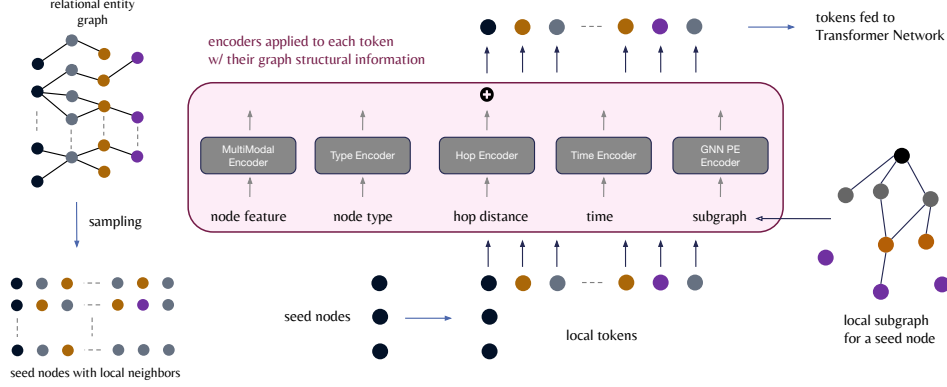
Figure 2: The tokenization procedure. A temporal-aware subgraph sampling step extracts a fixed set of local tokens for each training seed node, denoted by the node in black. Each token incorporates its respective graph structure information, which are element-wise transformed to a common embedding space and combined to form the effective token representation to be fed to the Transformer network.

ensuring that only nodes with timestamps $\tau(v_j) \leq \tau(v_i)$ are included to prevent temporal leakage. Each token in this set is represented by a **5-tuple**: $(x_{v_j}, \phi(v_j), p(v_i, v_j), \tau(v_j) - \tau(v_i), \text{GNN-PE}_{v_j})$, where, (i) node features (x_{v_j}) denotes the raw features derived from entity attributes in the database, (ii) node type ($\phi(v_j)$) is a categorical identifier corresponding to the entity's originating table, (iii) relative hop distance ($p(v_i, v_j)$) captures the structural distance between the seed node v_i and the neighbor node v_j, (iv) relative time ($\tau(v_j) - \tau(v_i)$) represents the temporal difference between the neighbor and seed node, and (v) finally, subgraph based PE (GNN-PE$_{v_j}$) provides a graph positional encoding for each node within the sampled subgraph, generated by applying a lightweight GNN to the subgraph's adjacency matrix with random node feature initialization [43, 26].

Encoders. Each element in the 5-tuple is processed by a specialized encoder before being combined into the final token representation, as illustrated in Figure 2.

*1. **Node Feature Encoder.*** The node features x_{v_j}, representing the columnar attributes of the node v_j in REG (which corresponds to a table row in a database), are encoded into a d-dimensional embedding. Each modality, such as numerical, categorical, multi-categorical, text, and image data, is encoded separately using modality-specific encoders following [19], and the resulting representations are then aggregated into a unified d-dimensional embedding.

$$h_{\text{feat}}(v_j) = \text{MultiModalEncoder}(x_{v_j}) \in \mathbb{R}^d \tag{1}$$

where MultiModalEncoder($\cdot$) is unified feature encoder adapted from [19].

*2. **Node Type Encoder.*** The node type encoding steps converts each table-specific entity type $\phi(v_j)$ to a d-dimensional representation, incorporating the heterogeneous information from the input data.

$$h_{\text{type}}(v_j) = W_{\text{type}} \cdot \text{onehot}(\phi(v_j)) \in \mathbb{R}^d \tag{2}$$

where $\phi(v_j)$ is the node type of v_j, $W_{\text{type}} \in \mathbb{R}^{d \times |T|}$ is the learnable weight matrix, $|T|$ is the number of node types, and onehot($\cdot$) is the one-hot encoding function.

*3. **Hop Encoder.*** The relative hop distance $p(v_i, v_j)$, that captures the structural proximity between the seed node v_i and a neighbor node v_j, is encoded into a d-dimensional embedding as:

$$h_{\text{hop}}(v_i, v_j) = W_{\text{hop}} \cdot \text{onehot}(p(v_i, v_j)) \in \mathbb{R}^d \tag{3}$$

with $p(v_i, v_j)$ being the relative hop distance between seed node v_i and neighbor node v_j, and $W_{\text{hop}} \in \mathbb{R}^{d \times h_{\max}}$ the learnable matrix mapping hop distances (up to $h_{\max}$).

*4. **Time Encoder.*** The time encoder linearly transforms the time difference $\tau(v_j) - \tau(v_i)$ between a neighbor node v_j and the seed node v_i:

$$h_{\text{time}}(v_i, v_j) = W_{\text{time}} \cdot (\tau(v_j) - \tau(v_i)) \in \mathbb{R}^d \tag{4}$$

where $\tau(v_j) - \tau(v_i)$ is the relative time difference, and $W_{\text{time}} \in \mathbb{R}^{d \times 1}$ are learnable parameters.
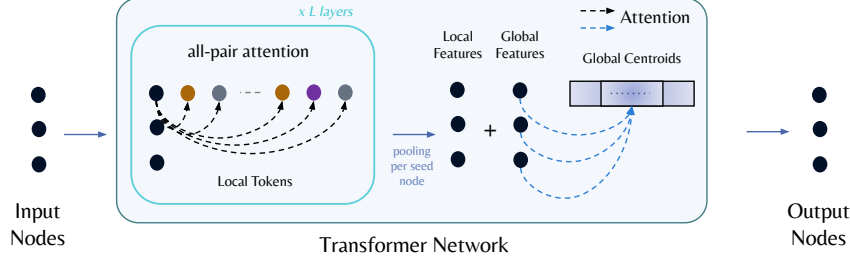
5

Figure 3: The Transformer network which processes the input tokens by first building local representations using the local tokens, then incorporating global context by attending to centroids that are dynamically updated during training. The final node representations combine both local structural details and global database context, enabling effective prediction across downstream tasks.

*5. **Subgraph PE Encoder.*** Finally, for capturing local graph structure that can otherwise not be represented by other elements of the token, we apply a light-weight GNN to the subgraph. This GNN encoder effectively preserves important structural relationships, such as complex cycles and quasi-cliques between entities [25], as well as parent-child relationships (e.g., a *product* node within the local subgraph corresponding to specific *transactions*), and can be written as:

$$h_{\text{pe}}(v_j) = \text{GNN}(A_{\text{local}}, Z_{\text{random}})_j \in \mathbb{R}^d \tag{5}$$

where $\text{GNN}(\cdot, \cdot)_j$ is a light-weight GNN applied to the local subgraph yielding the encoding for node v_j, $A_{\text{local}} \in \mathbb{R}^{K \times K}$ is the adjacency matrix of the sampled subgraph of K nodes, and $Z_{\text{random}} \in \mathbb{R}^{K \times d_{\text{init}}}$ are randomly initialized node features for the GNN (with d_{init} as the initial feature dimension).

One key advantage of using random node features in this GNN encoder is that it breaks structural symmetries between the subgraph topology and node attributes, thereby increasing the expressive power of GNN layers [43]. However, a fixed random initialization would destroy permutation equivariance which is a critical property for generalization. To address this challenge, we resample Z_{random} independently at every training step. This 'stochastic initialization' approach can be viewed as a relaxed version of the learnable PE method described in [26], thus approximately preserving permutation equivariance while retaining the expressivity gains afforded by the randomization.

At last, the effective token representation is formed by combining all encoded elements:

$$h_{\text{token}}(v_j) = O \cdot [h_{\text{feat}}(v_j) \, || \, h_{\text{type}}(v_j) \, || \, h_{\text{hop}}(v_i, v_j) \, || \, h_{\text{time}}(v_i, v_j) \, || \, h_{\text{pe}}(v_j)] \tag{6}$$

where $||$ denotes the concatenation of the individual encoder outputs, and $O \in \mathbb{R}^{5d \times d}$ is a learnable matrix to mix the embeddings. This multi-element approach provides a comprehensive token representation that explicitly captures node features, type information, structural position, temporal dynamics, and local topology without requiring expensive computation on the graph structure.

3.2 Transformer Network

The Transformer network in RELGT, shown in Figure 3, processes the tokenized relational entity graph using a combination of local and global attention mechanisms, following the successful design components used in modern GTs [41, 50, 30, 11].

Local module. The local attention mechanism allows each seed node to attend to its K local tokens selected during tokenization, capturing the fine-grained relationships defined by the database schema. This mechanism is different from a GNN used in RDL [42] in two key aspects: self-attention is used as the message-passing scheme and the attention is all-pair, *i.e.*, all nodes in the local K set attend to each other. This is implemented using an L layer Transformer network [47] and provides a broader structural coverage compared to a baseline GNN [42]. A practical application of this improvement can be seen in the e-commerce example introduced in Section 1, where the proposed full-attention mechanism can directly connect seemingly unrelated products by identifying relationships through shared transactions or customer behaviors. This capability enables the model to capture subtle associations, such as customers frequently purchasing unexpected combinations of items.

The local node representation $h_{\text{local}}(v_i)$ is obtained as:

$$h_{\text{local}}(v_i) = \text{Pool}(\text{FFN}(\text{Attention}(v_i, \{v_j\}_{j=1}^K))_L) \tag{7}$$

6

where, L denotes the layers, FFN and Attention are standard components in a Transformer [47], and Pool denotes the aggregation of $\{v_j\}_{j=1}^K$ and v_i using a learnable linear combination.

Global module. The global attention mechanism enables each seed node to attend to a set of B global tokens representing centroids of all nodes in the graph, conceptually and is adapted from prior works [30, 11]. These centroids are updated during training using an Exponential Moving Average (EMA) K-Means algorithm applied to seed node features in each mini-batch, providing a broader contextual view beyond the local neighborhood. The global representation is formulated as:

$$h_{\text{global}}(v_i) = \text{Attention}(v_i, \{c_b\}_{b=1}^B) \tag{8}$$

The final output representation of each node v_i is obtained by combining local and global embeddings:

$$h_{\text{output}}(v_i) = \text{FFN}([h_{\text{local}}(v_i) \,||\, h_{\text{global}}(v_i)]) \tag{9}$$

with FFN being a feed forward network. The components of the Transformer in all stages follow standard instantiations with normalization and residual connections.

For downstream prediction, the combined representation of the seed node is passed through a task-specific prediction head. The model is trained end-to-end using suitable task specific loss functions. By leveraging multi-element token representations within a hybrid local-global Transformer architecture, RELGT effectively addresses the challenges of heterogeneity, temporal dynamics, and schema-defined structures inherent in relational entity graphs.

4 Experiments

RELGT is evaluated on the recently introduced Relational Deep Learning Benchmark (RelBench) [42]. RelBench consists of 7 datasets from diverse relational database domains, including e-commerce, clinical records, social networks, and sports, among others. These datasets are curated from their respective source domains and consist a wide range of sizes, from 1.3K to 5.4M records in the training set for the prediction tasks, with a total of 47M training records. For each dataset, multiple predictive tasks are defined, such as predicting a user's engagement with an advertisement within the next four days or determining whether a clinical trial will achieve its primary outcome within the next year. In total, RelBench has 30 tasks across the 7 datasets, covering entity classification, entity regression, and recommendation. For our evaluation, we focus on 21 tasks on entity classification and regression [3].

4.1 Setup and Baselines

We implement RELGT within the RDL pipeline [42] by replacing the original GNN component, while preserving the learning mechanisms, database loaders, and task evaluators. The model has between 10-20 million parameters, and we use a learning rate of $1e-4$. For tasks with fewer than one million training nodes, we tune the number of layers $L \in 1, 4, 8$ and use dropout rates of $0.3, 0.4, 0.5$. For tasks with more than one million training nodes, we fix the number of layers to $L = 4$ due to compute budgets. For the sampling during the token preparation stage, we use $K = 300$ local neighbors and set $B = 4096$ as the number of tokens for global centroids. For smaller datasets (under one million training nodes), we use a batch size of 256 to ensure sufficient training steps. For larger datasets, we use a batch size of 1024. We do not perform exhaustive hyperparameter tuning; rather, our goal is to showcase the benefits of using RELGT in place of GNNs within the RDL framework. As shown in our ablation of the multi-element tokenization and global module in RELGT (Table 2), and context size (Figure 4), careful tuning may further improve performance across different tasks.

In addition to the HeteroGNN baseline used in RDL, we report results for two variants of the Heterogeneous Graph Transformer (HGT) [20] to highlight the advantages of RELGT over existing GT models. Notably, many GTs, such as GraphGPS [41], are not directly applicable to heterogeneous graphs. Therefore, we adopt HGT and an enhanced version, HGT+PE, which incorporates Laplacian positional encodings (LapPE). These positional encodings are computed on the sampled subgraphs rather than the entire graph. Additional implementation details are included in Appendix A.3.

---

[3]We exclude recommendation tasks in this work since they involve specific considerations, such as identifying target nodes [54] or using pair-wise learning architectures [55] and using RELGT trivially in RDL is sub-optimal.

Table 1: Test set results on the entity regression and classification tasks in RelBench. Best values are in **bold**. RDL: HeteroGNN baseline [42], HGT: Heterogeneous GT [20], PE: Laplacian Positional Encodings [10]. Relative gains are expressed as percentage improvement over RDL baseline.

(a) MAE for entity regression. Lower is better

Dataset	Task	RDL	HGT	HGT +PE	RelGT (ours)	% Rel. Gain
rel-f1	driver-position	4.022	4.1598	4.2358	**3.9170**	2.61
rel-avito	ad-ctr	0.041	0.0441	0.0494	**0.0345**	15.85
rel-event	user-attendance	0.258	0.2635	0.2562	**0.2502**	2.79
rel-trial	study-adverse	44.473	43.3253	**42.4622**	43.9923	1.08
	site-success	0.400	0.4374	0.4431	**0.3263**	18.43
rel-amazon	user-ltv	14.313	15.3804	15.9296	**14.2665**	0.32
	item-ltv	50.053	56.1384	55.6211	**48.9222**	2.26
rel-stack	post-votes	**0.065**	0.0679	0.0680	0.0654	-0.62
rel-hm	item-sales	0.056	0.0655	0.0641	**0.0536**	4.29

(b) AUC for entity classification. Higher is better.

Dataset	Task	RDL	HGT	HGT +PE	RelGT (ours)	% Rel. Gain
rel-f1	driver-dnf	0.7262	0.7142	0.7109	**0.7587**	4.48
	driver-top3	0.7554	0.6389	0.8340	**0.8352**	10.56
rel-avito	user-clicks	0.6590	0.6584	0.6387	**0.6830**	3.64
	user-visits	0.6620	0.6426	0.6507	**0.6678**	0.88
rel-event	user-repeat	**0.7689**	0.6717	0.6590	0.7609	-1.04
	user-ignore	0.8162	**0.8348**	0.8161	0.8157	-0.06
rel-trial	study-outcome	0.6860	0.5679	0.5691	**0.6861**	0.01
rel-amazon	user-churn	**0.7042**	0.6608	0.6589	0.7039	-0.04
	item-churn	**0.8281**	0.7824	0.7840	0.8255	-0.31
rel-stack	user-engagement	0.9021	0.8898	0.8852	**0.9053**	0.35
	user-badge	**0.8986**	0.8652	0.8518	0.8632	-3.94
rel-hm	user-churn	**0.6988**	0.6773	0.6491	0.6927	-0.87

4.2 Results and Discussion

RELGT improves over GNN in RDL. The experimental results in Tables 1a and 1b demonstrate that RELGT consistently matches or outperforms the standard GNN baseline used in RDL [42] across multiple datasets and tasks. We observe the largest improvements in `rel-trial site-success` (18.43%), `rel-avito ad-ctr` (15.85%), and `rel-f1 driver-top3` (10.56%), while on `rel-stack user-badge`, RELGT performs below the RDL baseline by a margin of -3.94%. For all other tasks, RELGT consistently improves or matches the performance of the baseline GNN. We attribute the overall performance improvement to two key factors: (i) the broader structural coverage enabled by RELGT's attention mechanisms as described in Section 3.2, and (ii) the fine-grained encodings employed in our tokenization scheme, which are further studied as follows and presented in Table 2.

Subgraph GNN PE is critical in RELGT. In Table 2, we highlight the importance of several components in RELGT by conducting ablation studies. We remove one component at a time while preserving all others, and report the relative performance drop compared to the full RELGT model. Our results show that removing the subgraph GNN (PE), which encodes local subgraph structure (Section 3.1), leads to consistent performance degradation across all tasks. This component proves critical for disambiguating parent-child relationships when full-attention is applied, thanks to the random node features initialization [43, 26]. For instance, without the GNN (PE), *products* belonging to specific *transactions* (Figure 1) cannot be effectively captured, even when other encodings remain.

Global module can bring gains depending on the task. In the same Table 2, our results of removing the global attention to the learnable centroids (Section 3.2) reveal task-dependent patterns that align with the findings reported in [30, 11]. For some tasks, such as `rel-trial site-success`, removing the attention to the centroids tokens leads to a substantial performance drop (-19.08%), indicating that the global database-wide context provides crucial information beyond the local neighborhood. However, for certain tasks such as `rel-avito user-clicks`, removing the global module actually improves performance (7.79% relative gain), suggesting that for some prediction targets, local information is sufficient, and the global context might introduce noise. These mixed results highlight the complementary nature of local and global information in relational graphs, with the latter being optional depending on the task.

Ablation of other encodings. The remaining ablations in Table 2 reveal mixed results across different components. While removing explicit fine-grained encodings (node type, hop distance, and relative time) degrades performance on some tasks, it improves performance on others. For tasks with specific temporal dependencies (as detailed in the Appendix A.1), our current temporal encodings may inadvertently introduce noise. Similarly, for node type and hop distance encodings, their information might already be partially captured by other model components. Despite these variations, the full RELGT model still shows consistently superior results when averaged across all tasks. However, our findings suggest that RELGT's performance could be further enhanced by careful tuning of these encoding components based on their task-specific importance. In particular, additional improvements can be achieved by incorporating more effective temporal encoding methods [7, 21, 23].

HGT, a GT baseline, underperforms with significant computational overhead. As shown in Tables 1a and 1b, HGT [20] underperforms compared to the HeteroGNN baseline of RDL [42] across

Table 2: Relative drop (%) in performance in RELGT after removing a model component. Negative scores suggest the component is critical in RELGT, and vice-versa. Full results in Table 7.

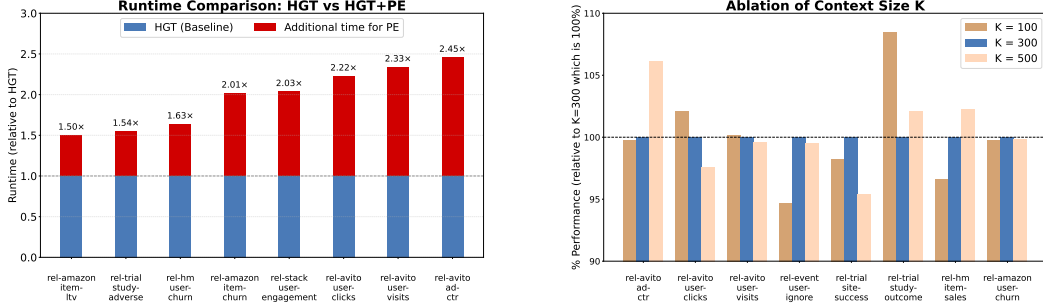| Dataset	Task	No Global Module	No GNN PE	No Node Type	No Hop Distance	No Relative Time
rel-avito	ad-ctr	−6.00	−1.14	−7.14	−3.43	−9.14
rel-avito	user-clicks	7.85	−15.15	5.01	5.77	8.37
rel-avito	user-visits	−0.35	−2.38	−0.11	0.39	−0.75
rel-event	user-ignore	−1.30	0.12	−0.11	0.66	−0.09
rel-trial	study-outcome	−2.14	−1.72	3.74	−0.43	2.48
rel-trial	site-success	−19.01	−9.17	−2.88	−21.49	−0.71
rel-amazon	user-churn	−0.64	−0.78	0.16	0.06	−2.20
rel-hm	item-sales	−9.33	−17.35	−12.69	0.93	−77.24
	Average	−3.87	−5.95	−1.75	−2.19	−9.91

Figure 4: *Left:* Epoch runtime comparison of HGT [20] and HGT+PE, with Laplacian PE (see Figure 5 for all tasks). The red portion shows the additional time consumed by the precomputation of Laplacian PE against the base HGT time (blue). *Right:* Ablation for different K values as the local context size in RELGT. Results using $K = 300$ serve as the baseline (100% performance), with $K = 100$ and $K = 500$ runs measured as % of performance relative to $K = 300$.

most tasks, with only two exceptions: `rel-trial study-adverse` and `rel-event user-ignore`. Notably, the integration of Laplacian eigenvectors as PEs in HGT improves performance in just 5 out of 21 tasks. Moreover, as illustrated in Figure 4, the computational overhead required for precomputing the Laplacian PEs substantially increases per-epoch runtime across various tasks. These empirical findings clearly reveal the difficulties of directly applying existing GT architectures to relational entity graphs, emphasizing the importance and need for our contributions with RELGT.

Local context size K. In our main RELGT experiments, we set the local context size at 300 nodes (Section 3.1), however, we study its variability in Figure 4 for context sizes $K \in \{100, 300, 500\}$. Although $K = 300$ generally produces the best results, optimal values vary across specific tasks. For instance, `rel-avito ad-ctr` benefits from a larger context size, whereas `rel-trial study-outcome` achieves better performance with a smaller context window. These findings suggest that RELGT's performance could be further enhanced by task-specific tuning of the context size, allowing for better model expressivity based on the structural characteristics of each dataset.

5 Conclusion

In this work, we introduce the first Graph Transformer designed specifically for relational entity graphs: the Relational Graph Transformer RELGT. It addresses key challenges faced by existing models, such as incorporating heterogeneity, temporality, and comprehensive structural modeling within a unified GT framework. RELGT represents nodes as multi-element tokens enriched with fine-grained graph context and combines local attention over sampled subgraph tokens with global attention to learnable centroids, enabling effective representation learning on relational data. Experiments on the RelBench benchmark show that RELGT consistently outperforms GNN and GT baselines across multiple tasks. Moreover, our analysis highlights the critical role of subgraph-based positional encodings as a lightweight and effective alternative to traditional graph positional encodings. This work establishes RELGT as a powerful architecture for relational deep learning and opens new avenues for advancing and scaling such architectures toward foundation models tailored for relational data.

Acknowledgments and Disclosure of Funding

References

[1] Uri Alon and Eran Yahav. On the bottleneck of graph neural networks and its practical implications. *arXiv preprint arXiv:2006.05205*, 2020.

[2] Michael M Bronstein, Joan Bruna, Taco Cohen, and Petar Veličković. Geometric deep learning: Grids, groups, graphs, geodesics, and gauges. *arXiv preprint arXiv:2104.13478*, 2021.

[3] Semih Cantürk, Renming Liu, Olivier Lapointe-Gagné, Vincent Létourneau, Guy Wolf, Dominique Beaini, and Ladislav Rampášek. Graph positional and structural encoder. *arXiv preprint arXiv:2307.07107*, 2023.

[4] Jinsong Chen, Kaiyuan Gao, Gaichao Li, and Kun He. Nagphormer: A tokenized graph transformer for node classification in large graphs. In *The Eleventh International Conference on Learning Representations*, 2022.

[5] Tianlang Chen, Charilaos Kanatsoulis, and Jure Leskovec. Relgnn: Composite message passing for relational deep learning. *arXiv preprint arXiv:2502.06784*, 2025.

[6] Tianqi Chen and Carlos Guestrin. Xgboost: A scalable tree boosting system. In *Proceedings of the 22nd acm sigkdd international conference on knowledge discovery and data mining*, pages 785–794, 2016.

[7] Aaron Clauset and Nathan Eagle. Persistence and periodicity in a dynamic proximity network. *arXiv preprint arXiv:1211.7343*, 2012.

[8] Edgar F Codd. A relational model of data for large shared data banks. *Communications of the ACM*, 13(6):377–387, 1970.

[9] Vijay Prakash Dwivedi and Xavier Bresson. A generalization of transformer networks to graphs. *AAAI Workshop on Deep Learning on Graphs: Methods and Applications*, 2021.

[10] Vijay Prakash Dwivedi, Chaitanya K Joshi, Anh Tuan Luu, Thomas Laurent, Yoshua Bengio, and Xavier Bresson. Benchmarking graph neural networks. *arXiv:2003.00982*, 2020.

[11] Vijay Prakash Dwivedi, Yozen Liu, Anh Tuan Luu, Xavier Bresson, Neil Shah, and Tong Zhao. Graph transformers for large graphs. *arXiv preprint arXiv:2312.11109*, 2023.

[12] Vijay Prakash Dwivedi, Anh Tuan Luu, Thomas Laurent, Yoshua Bengio, and Xavier Bresson. Graph neural networks with learnable structural and positional representations. In *International Conference on Learning Representations*, 2022.

[13] Matthias Fey, Weihua Hu, Kexin Huang, Jan Eric Lenssen, Rishabh Ranjan, Joshua Robinson, Rex Ying, Jiaxuan You, and Jure Leskovec. Position: Relational deep learning-graph representation learning on relational databases. In *Forty-first International Conference on Machine Learning*, 2024.

[14] Matthias Fey and Jan Eric Lenssen. Fast graph representation learning with pytorch geometric. *arXiv preprint arXiv:1903.02428*, 2019.

[15] Justin Gilmer, Samuel S Schoenholz, Patrick F Riley, Oriol Vinyals, and George E Dahl. Neural message passing for quantum chemistry. In *International conference on machine learning*, pages 1263–1272. PMLR, 2017.

[16] Aaron Grattafiori, Abhimanyu Dubey, Abhinav Jauhri, Abhinav Pandey, Abhishek Kadian, Ahmad Al-Dahle, Aiesha Letman, Akhil Mathur, Alan Schelten, Alex Vaughan, et al. The llama 3 herd of models. *arXiv preprint arXiv:2407.21783*, 2024.

[17] Aditya Grover and Jure Leskovec. node2vec: Scalable feature learning for networks. In *Proceedings of the 22nd ACM SIGKDD international conference on Knowledge discovery and data mining*, pages 855–864, 2016.

[18] Will Hamilton, Zhitao Ying, and Jure Leskovec. Inductive representation learning on large graphs. *Advances in neural information processing systems*, 30, 2017.

[19] Weihua Hu, Yiwen Yuan, Zecheng Zhang, Akihiro Nitta, Kaidi Cao, Vid Kocijan, Jinu Sunil, Jure Leskovec, and Matthias Fey. Pytorch frame: A modular framework for multi-modal tabular learning. *arXiv preprint arXiv:2404.00776*, 2024.

[20] Ziniu Hu, Yuxiao Dong, Kuansan Wang, and Yizhou Sun. Heterogeneous graph transformer. In *Proceedings of the web conference 2020*, pages 2704–2710, 2020.

[21] Shenyang Huang, Farimah Poursafaei, Reihaneh Rabbany, Guillaume Rabusseau, and Emanuele Rossi. Utg: Towards a unified view of snapshot and event based models for temporal graphs. *arXiv preprint arXiv:2407.12269*, 2024.

[22] Yinan Huang, William Lu, Joshua Robinson, Yu Yang, Muhan Zhang, Stefanie Jegelka, and Pan Li. On the stability of expressive positional encodings for graphs. In *The Twelfth International Conference on Learning Representations*.

[23] Xiangjian Jiang and Yanyi Pu. Exploring time granularity on temporal graphs for dynamic link prediction in real-world networks. *arXiv preprint arXiv:2311.12255*, 2023.

[24] Chaitanya Joshi. Transformers are graph neural networks. *The Gradient*, 12:17, 2020.

[25] Charilaos Kanatsoulis and Alejandro Ribeiro. Counting graph substructures with graph neural networks. In *The twelfth international conference on learning representations*, 2024.

[26] Charilaos I Kanatsoulis, Evelyn Choi, Stephanie Jegelka, Jure Leskovec, and Alejandro Ribeiro. Learning efficient positional encodings with graph neural networks. In *The Thirteenth International Conference on Learning Representations*.

[27] Guolin Ke, Qi Meng, Thomas Finley, Taifeng Wang, Wei Chen, Weidong Ma, Qiwei Ye, and Tie-Yan Liu. Lightgbm: A highly efficient gradient boosting decision tree. *Advances in neural information processing systems*, 30, 2017.

[28] Jinwoo Kim, Dat Nguyen, Seonwoo Min, Sungjun Cho, Moontae Lee, Honglak Lee, and Seunghoon Hong. Pure transformers are powerful graph learners. *Advances in Neural Information Processing Systems*, 35:14582–14595, 2022.

[29] Thomas N Kipf and Max Welling. Semi-supervised classification with graph convolutional networks. *arXiv preprint arXiv:1609.02907*, 2016.

[30] Kezhi Kong, Jiuhai Chen, John Kirchenbauer, Renkun Ni, C Bayan Bruss, and Tom Goldstein. Goat: A global transformer on large-scale graphs. In *International Conference on Machine Learning*, 2023.

[31] Devin Kreuzer, Dominique Beaini, Will Hamilton, Vincent Létourneau, and Prudencio Tossou. Rethinking graph transformers with spectral attention. *Advances in Neural Information Processing Systems*, 34:21618–21629, 2021.

[32] Veronica Lachi, Antonio Longa, Beatrice Bevilacqua, Bruno Lepri, Andrea Passerini, and Bruno Ribeiro. Over 100x speedup in relational deep learning via static gnns and tabular distillation. 2024.

[33] Derek Lim, Joshua David Robinson, Lingxiao Zhao, Tess Smidt, Suvrit Sra, Haggai Maron, and Stefanie Jegelka. Sign and basis invariant networks for spectral graph representation learning. In *The Eleventh International Conference on Learning Representations*, 2022.

[34] Andreas Loukas. What graph neural networks cannot learn: depth vs width. *arXiv preprint arXiv:1907.03199*, 2019.

[35] Qiheng Mao, Zemin Liu, Chenghao Liu, and Jianling Sun. Hinormer: Representation learning on heterogeneous information networks with graph transformer. In *Proceedings of the ACM web conference 2023*, pages 599–610, 2023.

[36] Grégoire Mialon, Dexiong Chen, Margot Selosse, and Julien Mairal. Graphit: Encoding graph structure in transformers. *arXiv preprint arXiv:2106.05667*, 2021.

[37] Christopher Morris, Martin Ritzert, Matthias Fey, William L Hamilton, Jan Eric Lenssen, Gaurav Rattan, and Martin Grohe. Weisfeiler and leman go neural: higher-order graph neural networks. In *Proceedings of the Thirty-Third AAAI Conference on Artificial Intelligence and Thirty-First Innovative Applications of Artificial Intelligence Conference and Ninth AAAI Symposium on Educational Advances in Artificial Intelligence*, pages 4602–4609, 2019.

[38] Luis Müller, Mikhail Galkin, Christopher Morris, and Ladislav Rampášek. Attending to graph transformers. *arXiv preprint arXiv:2302.04181*, 2023.

[39] A Paszke. Pytorch: An imperative style, high-performance deep learning library. *arXiv preprint arXiv:1912.01703*, 2019.

[40] Ştefan Postăvaru, Anton Tsitsulin, Filipe Miguel Gonçalves de Almeida, Yingtao Tian, Silvio Lattanzi, and Bryan Perozzi. Instantembedding: Efficient local node representations. *arXiv preprint arXiv:2010.06992*, 2020.

[41] Ladislav Rampášek, Michael Galkin, Vijay Prakash Dwivedi, Anh Tuan Luu, Guy Wolf, and Dominique Beaini. Recipe for a general, powerful, scalable graph transformer. *Advances in Neural Information Processing Systems*, 35:14501–14515, 2022.

[42] Joshua Robinson, Rishabh Ranjan, Weihua Hu, Kexin Huang, Jiaqi Han, Alejandro Dobles, Matthias Fey, Jan Eric Lenssen, Yiwen Yuan, Zecheng Zhang, et al. Relbench: A benchmark for deep learning on relational databases. *Advances in Neural Information Processing Systems*, 37:21330–21341, 2024.

[43] Ryoma Sato, Makoto Yamada, and Hisashi Kashima. Random features strengthen graph neural networks. In *Proceedings of the 2021 SIAM international conference on data mining (SDM)*, pages 333–341. SIAM, 2021.

[44] Michael Schlichtkrull, Thomas N Kipf, Peter Bloem, Rianne Van Den Berg, Ivan Titov, and Max Welling. Modeling relational data with graph convolutional networks. In *The semantic web: 15th international conference, ESWC 2018, Heraklion, Crete, Greece, June 3–7, 2018, proceedings 15*, pages 593–607. Springer, 2018.

[45] Hamed Shirzad, Ameya Velingker, Balaji Venkatachalam, Danica J Sutherland, and Ali Kemal Sinop. Exphormer: Sparse transformers for graphs. *arXiv preprint arXiv:2303.06147*, 2023.

[46] Maciej Sypetkowski, Frederik Wenkel, Farimah Poursafaei, Nia Dickson, Karush Suri, Philip Fradkin, and Dominique Beaini. On the scalability of gnns for molecular graphs. *Advances in Neural Information Processing Systems*, 37:19870–19906, 2024.

[47] Ashish Vaswani, Noam Shazeer, Niki Parmar, Jakob Uszkoreit, Llion Jones, Aidan N Gomez, Łukasz Kaiser, and Illia Polosukhin. Attention is all you need. *Advances in Neural Information Processing Systems*, 30, 2017.

[48] Petar Velickovic, Guillem Cucurull, Arantxa Casanova, Adriana Romero, Pietro Lio, Yoshua Bengio, et al. Graph attention networks. *stat*, 1050(20):10–48550, 2017.

[49] Xiao Wang, Houye Ji, Chuan Shi, Bai Wang, Yanfang Ye, Peng Cui, and Philip S Yu. Heterogeneous graph attention network. In *The world wide web conference*, pages 2022–2032, 2019.

[50] Qitian Wu, Wentao Zhao, Chenxiao Yang, Hengrui Zhang, Fan Nie, Haitian Jiang, Yatao Bian, and Junchi Yan. Sgformer: Simplifying and empowering transformers for large-graph representations. *Advances in Neural Information Processing Systems*, 36:64753–64773, 2023.

[51] Marek Wydmuch, Łukasz Borchmann, and Filip Graliński. Tackling prediction tasks in relational databases with llms. *arXiv preprint arXiv:2411.11829*, 2024.

[52] Keyulu Xu, Weihua Hu, Jure Leskovec, and Stefanie Jegelka. How powerful are graph neural networks? In *International Conference on Learning Representations*, 2019.

[53] Chengxuan Ying, Tianle Cai, Shengjie Luo, Shuxin Zheng, Guolin Ke, Di He, Yanming Shen, and Tie-Yan Liu. Do transformers really perform badly for graph representation? *Advances in Neural Information Processing Systems*, 34:28877–28888, 2021.

[54] Jiaxuan You, Jonathan M Gomes-Selman, Rex Ying, and Jure Leskovec. Identity-aware graph neural networks. In *Proceedings of the AAAI conference on artificial intelligence*, volume 35, pages 10737–10745, 2021.

[55] Yiwen Yuan, Zecheng Zhang, Xinwei He, Akihiro Nitta, Weihua Hu, Dong Wang, Manan Shah, Shenyang Huang, Blaž Stojanovič, Alan Krumholz, et al. Contextgnn: Beyond two-tower recommendation systems. *arXiv preprint arXiv:2411.19513*, 2024.

[56] Jiaqi Zhai, Lucy Liao, Xing Liu, Yueming Wang, Rui Li, Xuan Cao, Leon Gao, Zhaojie Gong, Fangda Gu, Michael He, et al. Actions speak louder than words: Trillion-parameter sequential transducers for generative recommendations. *arXiv preprint arXiv:2402.17152*, 2024.

[57] Zaixi Zhang, Qi Liu, Qingyong Hu, and Chee-Kong Lee. Hierarchical graph transformer with adaptive node sampling. *Advances in Neural Information Processing Systems*, 35:21171–21183, 2022.

[58] Jianan Zhao, Chaozhuo Li, Qianlong Wen, Yiqi Wang, Yuming Liu, Hao Sun, Xing Xie, and Yanfang Ye. Gophormer: Ego-graph transformer for node classification. *arXiv preprint arXiv:2110.13094*, 2021.

[59] Wenhao Zhu, Tianyu Wen, Guojie Song, Xiaojun Ma, and Liang Wang. Hierarchical transformer for scalable graph learning. *arXiv preprint arXiv:2305.02866*, 2023.

Table 3: Dataset and task statistics from RelBench used for our evaluation.

Dataset	Task	Task type	#Rows of training table			#Unique Entities	%train/test Entity Overlap
			Train	Validation	Test		
rel-amazon	user-churn	classification	4,732,555	409,792	351,885	1,585,983	88.0
	item-churn	classification	2,559,264	177,689	166,842	416,352	93.1
	user-ltv	regression	4,732,555	409,792	351,885	1,585,983	88.0
	item-ltv	regression	2,707,679	166,978	178,334	427,537	93.5
rel-avito	user-clicks	classification	59,454	21,183	47,996	66,449	45.3
	user-visits	classification	86,619	29,979	36,129	63,405	64.6
	ad-ctr	regression	5,100	1,766	1,816	4,997	59.8
rel-event	user-repeat	classification	3,842	268	246	1,514	11.5
	user-ignore	classification	19,239	4,185	4,010	9,799	21.1
	user-attendance	regression	19,261	2,014	2,006	9,694	14.6
rel-f1	driver-dnf	classification	11,411	566	702	821	50.0
	driver-top3	classification	1,353	588	726	134	50.0
	driver-position	regression	7,453	499	760	826	44.6
rel-hm	user-churn	classification	3,871,410	76,556	74,575	1,002,984	89.7
	item-sales	regression	5,488,184	105,542	105,542	105,542	100.0
rel-stack	user-engagement	classification	1,360,850	85,838	88,137	88,137	97.4
	user-badge	classification	3,386,276	247,398	255,360	255,360	96.9
	post-votes	regression	2,453,921	156,216	160,903	160,903	97.1
rel-trial	study-outcome	classification	11,994	960	825	13,779	0.0
	study-adverse	regression	43,335	3,596	3,098	50,029	0.0
	site-success	regression	151,407	19,740	22,617	129,542	42.0

A Appendix

A.1 Benchmark Details

In this section, we include the details on the datasets and the tasks in RelBench [42] which we use for our evaluation. RelBench consists of 7 datasets from diverse relational database domains, including e-commerce, clinical records, social networks, and sports, among others. These datasets are curated from their respective source domains and consist a wide range of sizes, from 1.3K to 5.4M records in the training set for the prediction tasks, with a total of 47M training records. For each dataset, multiple predictive tasks are defined, such as predicting a user's engagement with an advertisement within the next four days or determining whether a clinical trial will achieve its primary outcome within the next year. In total, RelBench has 30 tasks across the 7 datasets, covering entity classification, entity regression, and recommendation. For our evaluation, we focus on 21 tasks on entity classification and regression as RELGT primarily serves as a node representation learning model in RDL. We exclude recommendation tasks in this work since they involve specific considerations, such as identifying target nodes [54] or using pair-wise learning architectures [55] and using RELGT trivially in RDL is sub-optimal. We detail the dataset and task statistics in Table 3.

A.1.1 Datasets

rel-amazon. The Amazon E-commerce dataset consists of product details, user information, and review interactions from Amazon's platform, including metadata like pricing and categories, along with review ratings and content.

rel-avito. Avito's marketplace dataset contains search queries, advertisement characteristics, and contextual information from this major online trading platform that facilitates transactions across various categories including real estate and vehicles.

rel-event. The Event Recommendation dataset from Hangtime mobile app tracks users' social planning, capturing interactions, event details, demographic data, and social connections to reveal how relationships impact user behavior.

rel-f1. The F1 dataset provides comprehensive Formula 1 racing information since 1950, documenting drivers, constructors, manufacturers, and circuits with detailed records of race results, standings, and specific data on various racing sessions and pit stops.

`rel-hm.` H&M's dataset contains customer-product interactions from their e-commerce platform, featuring customer demographics, product descriptions, and purchase histories.

`rel-stack.` The Stack Exchange dataset documents activity from this network of Q&A websites, including user biographies, posts, comments, edits, votes, and question relationships where users earn reputation through contributions.

`rel-trial.` The clinical trial dataset from the AACT initiative has study protocols and outcomes, containing trial designs, participant information, intervention details, and results metrics, serving as a key resource for medical research.

A.1.2 Tasks

The following entity classification and regression tasks are defined in RelBench for the above datasets.

1. `rel-amazon`
   (a) `user-churn`: Predict whether a user will discontinue reviewing products within the next three months.
   (b) `item-churn`: Predict if a product will have no reviews in the next three months.
   (c) `user-ltv`: Estimate the total monetary value of merchandise in dolloar that a user will purchase and review within the next three months.
   (d) `item-ltv`: Estimate the total monetary value of purchases and reviews a product will receive during the next three months.

2. `rel-avito`
   (a) `user-visits`: Predict if a user will engage with several (advertisements) ads within the upcoming four days.
   (b) `user-clicks`: Predict whether a user will interact with multiple ads through clicking within the upcoming four days.
   (c) `ad-ctr`: Estimate the interaction probability for an ad, assuming it receives an interaction within four days.

3. `rel-event`
   (a) `user-attendance`: Estimate the number of of events a user will confirm attendance to (RSVP yes or maybe) within the upcoming seven days.
   (b) `user-repeat`: Predict whether a user will join an event (RSVP yes or maybe) within the upcoming seven days, provided they attended in an event during the previous fourteen days.
   (c) `user-ignore`: Predict whether a user will disregard or ignore more than two events invitations within the upcoming seven days.

4. `rel-f1`
   (a) `driver-dnf`: Predict if a driver will not finish a race within the upcoming month.
   (b) `driver-top3`: Determine if a driver will achieve a top-three qualifying position in a race within the upcoming month.
   (c) `driver-position`: Estimate a driver's average finishing placement across all races in the upcoming two months.

5. `rel-hm`
   (a) `user-churn`: Predict whether a customer will not perform any transactions in the upcoming week.
   (b) `item-sales`: Estimate total revenue generated by a product in the upcoming week.

6. `rel-stack`
   (a) `user-engagement`: Predict whether a user will contribute through voting, posting, or commenting within the upcoming three months.
   (b) `user-badge`: Predict whether a user will secure a new badge within the upcoming three months.

Table 4: Study of node initialization in Subgraph GNN PE. Relative drop is expressed as percentage drop of using Z_{LapPE} vs. Z_{random} and runtime ratio compares the time for Z_{LapPE} vs. Z_{random}.

Dataset	Task (# train)		Performance		% Rel Drop	Epoch time (m)		Runtime Ratio
		MAE ↓	Z_{random}	Z_{LapPE}		Z_{random}	Z_{LapPE}	
rel-avito	ad-ctr	Test	**0.035**	0.0369	-5.43	0.76	2.57	3.38
		Val	0.0314	0.0314				
rel-trial	site-success	Test	**0.326**	0.3452	-5.89	32.88	36.09	1.1
		Val	0.359	0.3683				
rel-hm	item-sales	Test	**0.0536**	0.0573	-6.9	49.26	53.8	1.09
		Val	0.0627	0.0667				

Dataset	Task (# train)		AUC ↑	Z_{random}	Z_{LapPE}	% Rel Drop	Z_{random}	Z_{LapPE}	Runtime Ratio
rel-avito	user-clicks	Test		**0.607**	0.583	-3.95	6.42	7.43	1.16
		Val		0.656	0.6564				
	user-visits	Test		**0.664**	0.6626	-0.21	9.26	10.50	1.13
		Val		0.699	0.7002				
rel-event	user-ignore	Test		**0.8**	0.7988	-0.15	1.85	2.77	1.5
		Val		0.881	0.8916				
rel-trial	study-outcome	Test		**0.674**	0.6532	-3.09	1.41	1.52	1.08
		Val		0.689	0.6719				
rel-amazon	user-churn	Test		0.7039	**0.7044**	0.07	168.00	170.55	1.02
		Val		0.7036	0.7036				

    (c) post-votes: Estimate the number of votes a user's post will accumulate over the upcoming three months.

7. rel-trial

    (a) study-outcome: Predict whether a clinical trial will achieve its principal outcome within the upcoming year.

    (b) study-adverse: Estimate the number of patients who will experience significant adverse effects or mortality in a clinical trial over the upcoming year.

    (c) site-success: Estimate the success rate of a clinical trial site in the upcoming year.

A.2   Node initialization for Subgraph GNN PE in RELGT

As described in Section 3.1, we employ a lightweight GNN PE to capture local graph structures that cannot be represented by other elements of the token, particularly the parent-child relationships among nodes in the local subgraph. The GNN is implemented as:

$$h_{\text{pe}}(v_j) = \text{GNN}(A_{\text{local}}, Z_{\text{random}})_j \in \mathbb{R}^d \tag{10}$$

where $\text{GNN}(\cdot, \cdot)_j$ is a lightweight GNN applied to the local subgraph, yielding the encoding for node v_j. Here, $A_{\text{local}} \in \mathbb{R}^{K \times K}$ represents the adjacency matrix of the sampled subgraph containing K nodes, and $Z_{\text{random}} \in \mathbb{R}^{K \times d_{\text{init}}}$ denotes randomly initialized node features for the GNN (with d_{init} as the initial feature dimension). In RELGT, we set $d_{\text{init}} = 1$.

The randomly initialized node features (Z_{random}) provide enhanced properties as discussed in Section 3.1. We investigate the alternative approach of using Laplacian PE (Z_{LapPE}) computed over the subgraph instead of random initialization and report these results in Table 4. For these results, we utilized a positional encoding dimension size of 4. Our findings indicate that Z_{LapPE} consistently underperforms compared to Z_{random}, while also introducing additional computational overhead ranging from $1.02\times$ to $3.38\times$ across the 8 selected tasks in our study. This shows the challenges of using existing PEs such as Laplacian PE in relational entity graphs and signify the use of GNN PE as part of RELGT's tokenization strategy.

A.3   HGT Baseline

In the main experiments (Section 4), we use the Heterogeneous Graph Transformer (HGT) [20] as a graph transformer (GT) baseline, and report results for two variants to demonstrate the advantages of RELGT over existing GT models. Specifically, we consider the standard HGT model and an
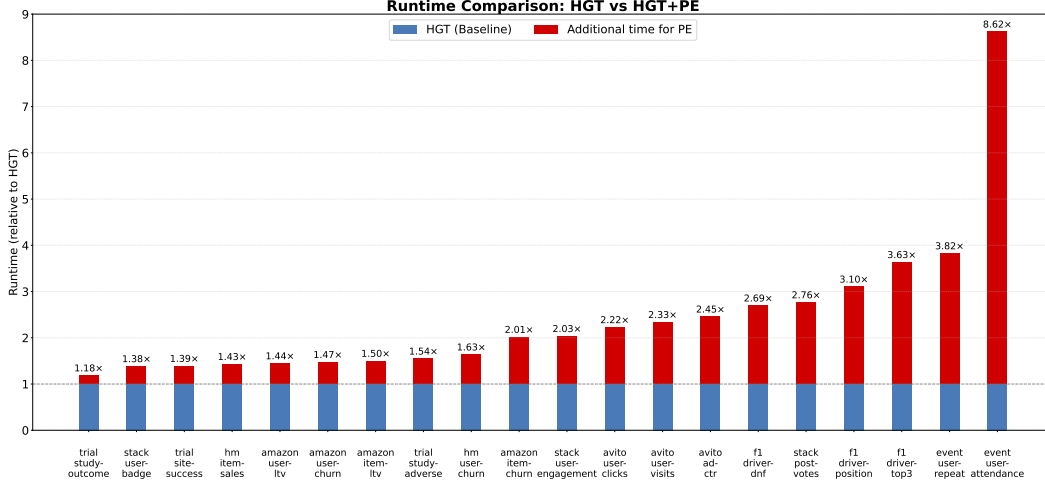
Figure 5: Runtime Comparison of HGT and HGT+PE baseline. Adding the Laplacian Positional Encoding increases computational overhead, with penalties on average training time per epoch. The overhead for PE reaches up to 761% relative to the training time of HGT on the same dataset.

enhanced version, HGT+PE, which incorporates Laplacian positional encodings (LapPE). These positional encodings are computed on sampled subgraphs rather than the full graph.

For implementation, we use the `HGTConv` layer from PyTorch Geometric [14] and integrate it into the RDL pipeline [42] by replacing the default GNN module. Both variants use 4 attention heads and 2 layers, similar to the configuration of the GNN module in RDL, with residual connections and layer normalization applied between layers. For the HGT+PE variant, we use LapPE of dimension 4 for all tasks, except for `rel-amazon item-ltv` and `rel-hm item-sales`, where we use dimension 2. Notably, because the relational entity graphs are heterogeneous, the Laplacian positional encodings is computed multiple times for each node type, unlike the original homogeneous setting for which LapPE was designed [10].

In addition to the main results in Table 1, we report per-epoch runtimes in Figure 5 and Table 5. We observe a significant computational overhead from precomputing Laplacian positional encodings, with slowdowns ranging from 1.8× to 8.62×, highlighting the challenge of directly applying existing graph PE techniques *as is* to relational entity graphs, and signifying the contributions of RELGT.

A.4 Detailed Results

In Table 6, we report the full results of different configurations we tuned for RELGT, particularly on the smaller datasets with lesser than a million training nodes. Table 7 provides the full scores for the RELGT component study in Table 2, while Table 8 provides the supporting results for Figure 4. Finally, we provide the elaborated version of the Tables 1a and 1b in Tables 9 and 9, respectively.

A.5 Resource Information.

We implement RELGT using PyTorch framework [39], PyTorch Geometric framework [14] and adapt the codebase of relational deep learning [42] `https://github.com/snap-stanford/relbench`. All our experiments are conducted on an NVIDIA A100 GPU server with 8 GPU nodes.

Table 5: Relative performance drop (%) when position encoding (PE) is removed from HGT+PE models and average training time per epoch of HGT and HGT+PE. Negative scores suggest the PE is critical, and vice-versa. HGT+PE consistently requires more training time per epoch compared to HGT without PE across all datasets.

Dataset	Task	No PE	HGT(s)	HGT+PE(s)
rel-f1	driver-position	1.79	1.47	4.56
rel-avito	ad-ctr	10.73	1.63	4.00
rel-event	user-attendance	−2.85	4.36	37.57
rel-trial	study-adverse	−2.03	9.72	15.02
rel-trial	site-success	1.29	45.73	63.41
rel-amazon	user-ltv	3.45	73.59	106.21
rel-amazon	item-ltv	−0.93	73.68	110.33
rel-stack	post-votes	0.15	191.23	528.25
rel-hm	item-sales	−2.18	94.66	135.05
rel-f1	driver-dnf	0.46	2.54	6.84
rel-f1	driver-top3	−23.39	0.38	1.38
rel-avito	user-clicks	3.08	11.09	24.66
rel-avito	user-visits	−1.24	17.16	40.07
rel-event	user-repeat	1.93	1.35	5.16
rel-event	user-ignore	2.29	4.49	651.10
rel-trial	study-outcome	−0.21	4.09	4.83
rel-amazon	user-churn	0.29	78.56	115.53
rel-amazon	item-churn	−0.20	75.51	152.06
rel-stack	user-engagement	0.52	175.16	356.07
rel-stack	user-badge	1.57	153.68	212.21
rel-hm	user-churn	4.34	77.73	127.04
	Average	−0.05	52.28	128.64

Table 6: RELGT results using $L \in 1, 4, 8$ and dropout $\in 0.3, 0.4, 0.5$ for the smaller datasets with less than a million training nodes.

Dataset	Task (# train)	MAE ↓	L1 0.3	L1 0.4	L1 0.5	L4 0.3	L4 0.4	L4 0.5	L8 0.3	L8 0.4	L8 0.5
rel-f1	driver-position (7k)	Test	4.942	5.6431	**3.917**	4.6316	4.0851	4.0042	5.5273	5.5569	4.6085
		Val	3.1897	3.1817	3.3257	3.1046	3.3352	3.1276	3.1589	3.2907	3.1843
rel-avito	ad-ctr (5k)	Test	0.0358	0.0352	**0.0345**	0.035	0.0366	0.038	0.0354	0.0358	0.0356
		Val	0.0322	0.0313	0.0314	0.0314	0.0322	0.0335	0.0317	0.0322	0.0324
rel-event	user-attendance (19k)	Test	0.2635	0.2595	0.2635	**0.2502**	0.2543	0.2584	0.2635	0.2637	0.2635
		Val	0.2618	0.2558	0.2618	0.2548	0.2534	0.253	0.2618	0.2599	0.2618
rel-trial	study-adverse (43k)	Test	44.8553	44.2260	44.848	44.8893	44.4310	**43.9923**	44.2245	44.5878	44.5013
		Val	46.3538	46.3193	46.2056	46.1031	45.9498	46.2148	46.1804	46.1381	46.4332
	site-success (151k)	Test	0.3490	0.3652	0.3830	0.4019	0.386	**0.3262**	0.3783	0.3431	0.3644
		Val	0.3493	0.3455	0.3550	0.3771	0.392	0.3593	0.3848	0.3643	0.3669

Dataset	Task (# train)	AUC ↑	L1 0.3	L1 0.4	L1 0.5	L4 0.3	L4 0.4	L4 0.5	L8 0.3	L8 0.4	L8 0.5
rel-f1	driver-dnf (11k)	Test	0.7434	0.7587	0.7521	**0.7587**	0.745	0.6957	0.7349	0.7393	0.741
		Val	0.6877	0.6761	0.6896	0.6804	0.6762	0.6768	0.6702	0.6803	0.6865
	driver-top3 (1k)	Test	0.7845	0.8203	0.8	0.8171	0.8157	**0.8352**	0.7871	0.8217	0.8222
		Val	0.7775	0.783	0.7764	0.7841	0.79	0.7958	0.7893	0.7847	0.7829
rel-avito	user-clicks (59k)	Test	0.6524	0.6233	0.6212	0.6067	0.5893	0.596	0.6245	**0.683**	0.6507
		Val	0.6649	0.6616	0.6501	0.6564	0.6608	0.6579	0.6587	0.6649	0.6648
	user-visits (86k)	Test	0.6627	0.6663	0.665	0.6615	0.6584	0.6642	0.6647	**0.6678**	0.664
		Val	0.7005	0.6993	0.7001	0.6954	0.6958	0.699	0.6995	0.7024	0.7011
rel-event	user-repeat (3k)	Test	0.6981	0.7403	0.7452	0.7563	0.7236	0.7432	**0.7609**	0.7316	0.7418
		Val	0.7172	0.7386	0.7319	0.7245	0.7207	0.736	0.7285	0.7209	0.7064
	user-ignore (19k)	Test	0.8006	0.802	0.7986	0.799	0.787	0.8002	0.7956	0.8076	**0.8157**
		Val	0.8739	0.8721	0.8729	0.878	0.8731	0.881	0.8757	0.8801	0.8868
rel-trial	study-outcome (11k)	Test	0.6808	0.6753	0.6837	0.6488	0.6818	0.6744	**0.6861**	0.6562	0.6649
		Val	0.6815	0.6792	0.6751	0.6737	0.676	0.689	0.6678	0.6746	0.6768

Table 7: Relative drop (%) in performance in RELGT after removing a model component. Negative scores suggest the component is critical in RELGT, and vice-versa.

Dataset	Task (# train)	MAE ↓	RelGT (Full)	RelGT (No Global)	% Rel. Drop	RelGT (No GNN)	% Rel. Drop	RelGT (No Type)	% Rel. Drop	RelGT (No Hop)	% Rel. Drop	RelGT (No Time)	% Rel. Drop
rel-avito	ad-ctr	Test	**0.0350**	0.0371	-6.0	0.0354	-1.14	0.0375	-7.14	0.0362	-3.43	0.0382	-9.14
		Val	0.0314	0.0323		0.0315		0.0328		0.0322		0.0337	
rel-trial	site-success	Test	**0.3262**	0.3882	-19.01	0.3561	-9.17	0.3356	-2.88	0.3963	-21.49	0.3285	-0.71
		Val	0.3593	0.3342		0.3637		0.3655		0.3614		0.3615	
rel-hm	item-sales	Test	**0.0536**	0.0586	-9.33	0.0629	-17.35	0.0604	-12.69	**0.0531**	0.93	0.095	-77.24
		Val	0.0627	0.0676		0.073		0.0696		0.0623		0.1025	

Dataset	Task (# train)	AUC ↑	RelGT (Full)	RelGT (No Global)	% Rel. Drop	RelGT (No GNN)	% Rel. Drop	RelGT (No Type)	% Rel. Drop	RelGT (No Hop)	% Rel. Drop	RelGT (No Time)	% Rel. Drop
rel-avito	user-clicks	Test	0.6067	0.6543	7.85	0.5148	-15.15	0.6371	5.01	0.6417	5.77	**0.6575**	8.37
		Val	0.6564	0.6496		0.6551		0.6559		0.6482		0.6579	
	user-visits	Test	0.6642	0.6619	-0.35	0.6484	-2.38	0.6635	-0.11	**0.6668**	0.39	0.6592	-0.75
		Val	0.699	0.6892		0.6879		0.6991		0.7016		0.7005	
rel-event	user-ignore	Test	0.8002	0.7898	-1.3	0.8012	0.12	0.7993	-0.11	**0.8055**	0.66	0.7995	-0.09
		Val	0.881	0.8575		0.8637		0.8873		0.8852		0.8789	
rel-trial	study-outcome	Test	0.6744	0.66	-2.14	0.6628	-1.72	**0.6996**	3.74	0.6715	-0.43	0.6911	2.48
		Val	0.689	0.664		0.6775		0.6728		0.6705		0.6578	
rel-amazon	user-churn	Test	0.7039	0.6994	-0.64	0.6984	-0.78	**0.705**	0.16	0.7043	0.06	0.6884	-2.2
		Val	0.7036	0.6994		0.6994		0.7042		0.704		0.6882	

Table 8: Ablation of context size K in RELGT.

Dataset	Task (# train)	MAE ↓	RELGT K=100	RELGT K=300	RELGT K=500
rel-avito	ad-ctr	Test	0.0375	0.0374	**0.0351**
		Val	0.0329	0.0319	0.031
rel-trial	site-success	Test	0.3739	**0.3674**	0.3842
		Val	0.3708	0.372	0.376
rel-hm	item-sales	Test	0.055	0.0532	**0.052**
		Val	0.0643	0.0619	0.061

Dataset	Task (# train)	AUC ↑	RelGT K=100	RelGT K=300	RelGT K=500
rel-avito	user-clicks	Test	**0.6628**	0.6491	0.6334
		Val	0.6437	0.6622	0.6632
	user-visits	Test	**0.6664**	0.6653	0.6627
		Val	0.7013	0.701	0.7005
rel-event	user-ignore	Test	0.7674	**0.8105**	0.8068
		Val	0.8682	0.8853	0.8843
rel-trial	study-outcome	Test	**0.7078**	0.6526	0.666
		Val	0.6575	0.663	0.6877
rel-amazon	user-churn	Test	0.7038	**0.7054**	0.7043
		Val	0.7033	0.7044	0.7042

Table 9: Results on the entity regression tasks in RelBench. Lower is better. Best values are in **bold**. Relative gains are expressed as percentage improvement over RDL baseline.

Dataset	Task	MAE ↓	RDL Baseline	HGT	HGT +PE	RelGT (ours)	% Rel. Gain
rel-f1	driver-position	Test	4.022	4.1598	4.2358	**3.9170**	2.61
		Val	3.193	3.3517	2.9894	3.3257	
rel-avito	ad-ctr	Test	0.041	0.0441	0.0494	**0.0345**	15.85
		Val	0.037	0.0409	0.0456	0.0314	
rel-event	user-attendance	Test	0.258	0.2635	0.2562	**0.2502**	2.79
		Val	0.255	0.2617	0.2574	0.2548	
rel-trial	study-adverse	Test	44.473	43.3253	**42.4622**	43.9923	1.08
		Val	46.290	45.9957	45.7966	46.2148	
	site-success	Test	0.400	0.4374	0.4431	**0.3263**	18.43
		Val	0.401	0.4198	0.4245	0.3593	
rel-amazon	user-ltv	Test	14.313	15.3804	15.9296	**14.2665**	0.32
		Val	12.132	13.1017	13.5599	12.1151	
	item-ltv	Test	50.053	56.1384	55.6211	**48.9222**	2.26
		Val	45.1401	51.2139	50.3468	43.8161	
rel-stack	post-votes	Test	**0.065**	0.0679	0.0680	**0.0654**	-0.62
		Val	0.059	0.0617	0.0618	0.0592	
rel-hm	item-sales	Test	0.056	0.0655	0.0641	**0.0536**	4.29
		Val	0.065	0.0749	0.0735	0.0627	

Table 10: Results on the entity classification tasks in RelBench. Higher is better. Best values are in **bold**. Relative gains are expressed as percentage improvement over RDL baseline.

Dataset	Task	AUC ↑	RDL Baseline	HGT	HGT +PE	RelGT (ours)	% Rel. Gain
rel-f1	driver-dnf	Test	0.7262	0.7142	0.7109	**0.7587**	4.48
		Val	0.7136	0.7678	0.7318	0.6804	
	driver-top3	Test	0.7554	0.6389	0.8340	**0.8352**	10.56
		Val	0.7764	0.6659	0.6079	0.7958	
rel-avito	user-clicks	Test	0.6590	0.6584	0.6387	**0.6830**	3.64
		Val	0.6473	0.5977	0.5656	0.6649	
	user-visits	Test	0.6620	0.6426	0.6507	**0.6678**	0.88
		Val	0.6965	0.6696	0.6732	0.7024	
rel-event	user-repeat	Test	**0.7689**	0.6717	0.6590	0.7609	-1.04
		Val	0.7125	0.6247	0.5974	0.7285	
	user-ignore	Test	0.8162	**0.8348**	0.8161	0.8157	-0.06
		Val	0.9170	0.8896	0.8940	0.8868	
rel-trial	study-outcome	Test	0.6860	0.5679	0.5691	**0.6861**	0.01
		Val	0.6818	0.5985	0.5925	0.6678	
rel-amazon	user-churn	Test	**0.7042**	0.6608	0.6589	0.7039	-0.04
		Val	0.7045	0.6639	0.6622	0.7036	
	item-churn	Test	**0.8281**	0.7824	0.7840	0.8255	-0.31
		Val	0.8239	0.7845	0.7846	0.8220	
rel-stack	user-engagement	Test	0.9021	0.8898	0.8852	**0.9053**	0.35
		Val	0.9059	0.8914	0.8847	0.9033	
	user-badge	Test	**0.8986**	0.8652	0.8518	0.8632	-3.94
		Val	0.8886	0.8760	0.8691	0.8741	
rel-hm	user-churn	Test	**0.6988**	0.6773	0.6491	0.6927	-0.87
		Val	0.7042	0.6814	0.6502	0.6988	